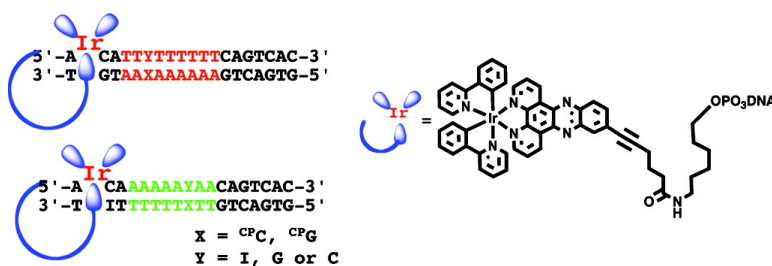


Long-Range Electron and Hole Transport through DNA with Tethered Cyclometalated Iridium(III) Complexes

Fangwei Shao, and Jacqueline K. Barton

J. Am. Chem. Soc., **2007**, 129 (47), 14733-14738 • DOI: 10.1021/ja0752437

Downloaded from <http://pubs.acs.org> on February 9, 2009



More About This Article

Additional resources and features associated with this article are available within the HTML version:

- Supporting Information
- Links to the 3 articles that cite this article, as of the time of this article download
- Access to high resolution figures
- Links to articles and content related to this article
- Copyright permission to reproduce figures and/or text from this article

[View the Full Text HTML](#)

Long-Range Electron and Hole Transport through DNA with Tethered Cyclometalated Iridium(III) Complexes

Fangwei Shao and Jacqueline K. Barton*

Contribution from the Division of Chemistry and Chemical Engineering, California Institute of Technology, Pasadena, California 91125

Received July 13, 2007; E-mail: jkbaron@caltech.edu

Abstract: A cyclometalated complex of Ir(III) is covalently tethered to DNA oligonucleotides and serves as both a photooxidant and photoreductant in the study of DNA-mediated hole transport (HT) and electron transport (ET). Spectroscopic and melting temperature studies support intercalation of the tethered complex into the DNA duplex through the functionalized dpdz ligand. Using these tethered assemblies, ET and HT is initiated in DNA by the same photoredox probe. Cyclopropylamine substituted bases, N₄-cyclopropylcytosine (^{CP}C) and N₂-cyclopropylguanine (^{CP}G) are used as kinetically fast electron and hole traps to probe the resulting electron migration processes after direct irradiation of the tethered Ir assembly. Oxidation of ^{CP}G and ^{CP}C is promoted efficiently by HT from photoexcited Ir(III) when the modified bases are positioned in the purine strands of the A-tract. In contrast, when ^{CP}C is embedded in a pyrimidine tract, ET to yield reductive decomposition is observed. Thus, the Ir(III)-tethered DNA assembly containing cyclopropyl-modified bases provides a unique model system to explore the two DNA-mediated electron migration processes using the same photoredox probe and the same DNA bridge.

Introduction

The structural core of a DNA duplex is constituted by an array of heterocyclic aromatic nucleic acid base pairs. This well-defined π -stacked structure provides an efficient pathway for charge migration, both hole transport (HT) and electron transport (ET).^{1,2} In HT, a radical cation, an electron hole, is injected and migrates through the DNA duplex to oxidize distant bases. On the other hand, ET occurs with DNA reduction and an excess electron is transported along the double helix.

DNA-mediated HT has been extensively explored using a variety of photooxidants and hole traps with both biochemical and spectroscopic assays.^{1–10} A conformationally gated domain model has been proposed by our laboratory to reconcile most of the experimental data that have been obtained.^{11,12} It has become increasingly clear that the interaction mode of photo-

oxidants with the DNA duplex is one of the essential factors in terms of studying HT mechanisms. For example, two fluorescent adenine analogues, 2-aminopurine (Ap) and 1,N₆-ethenoadenine (A_e) with similar reactivity to oxidize guanine, yield striking differences in distance dependence of HT.¹³ The distinctly low HT efficiency triggered by A_e is due to the significantly poor base stacking of the sterically bulky analogue within the double helix. With covalently tethered Rh(III) and Ru(II) complexes, which have extended intercalative ligands to achieve effective electronic coupling with DNA, efficient HT over at least 200 Å in DNA is observed.⁴ Thus, the critical ways in which photooxidants interact with the DNA helix can result in significant differences in HT.¹⁴

It has also become apparent that DNA-mediated HT yields different features when probed on different time scales.^{9a,14,15} Owing to its long ms lifetime, the guanine radical cannot report HT events on a fast time scale,¹⁶ leaving time for back electron transfer to occur. The development of cyclopropylamine-substituted bases, such as N₂-cyclopropylguanine (^{CP}G)¹⁷ and

- (1) (a) Delaney, S.; Barton, J. K. *J. Org. Chem.* **2003**, *68*, 6475–6483. (b) O'Neill, M. A.; Barton, J. K. *Charge Transfer in DNA: From Mechanism to Application*; Wagenknecht, H. A., Ed.; Wiley: New York, 2005; 27–75.
- (2) *Long-range electron transfer in DNA*, 1st ed.; Schuster, G. B., Ed.; Topics in Current Chemistry; Springer: 2004; p 236.
- (3) Hall, D. B.; Holmlin, R. E.; Barton, J. K. *Nature* **1996**, *382*, 731–735.
- (4) Núñez, M. E.; Hall, D. B.; Barton, J. K. *Chem. Biol.* **1999**, *6*, 85–97.
- (5) Henderson, P. T.; Jones, D.; Hampikian, G.; Kan, Y. Z.; Schuster, G. *Proc. Natl. Acad. Sci. U.S.A.* **1999**, *96*, 8353–8358.
- (6) Giese, B. *Annu. Rev. Biochem.* **2002**, *71*, 51–70.
- (7) Takada, T.; Kawai, K.; Cai, X.; Sugimoto, A.; Fujitsuka, M.; Majima, T. *J. Am. Chem. Soc.* **2004**, *126*, 1125–1129.
- (8) Nakatani, K.; Dohno, C.; Saito, I. *J. Am. Chem. Soc.* **2000**, *122*, 5893–5894.
- (9) (a) Yoo, J.; Delaney, S.; Stemp, E. D. A.; Barton, J. K. *J. Am. Chem. Soc.* **2003**, *125*, 6640–6641. (b) Delaney, S.; Yoo, J.; Stemp, E. D. A.; Barton, J. K. *Proc. Nat. Acad. Sci. U.S.A.* **2004**, *101*, 10511–10516.
- (10) Lewis, F. D.; Lestingier, R. L.; Wasielewski, M. R. *Acc. Chem. Res.* **2001**, *34*, 159–170.
- (11) (a) O'Neill, M. A.; Barton, J. K. *J. Am. Chem. Soc.* **2004**, *126*, 11471–11483. (b) O'Neill, M. A.; Barton, J. K. *J. Am. Chem. Soc.* **2004**, *126*, 13234–13235.

- (12) O'Neill, M. A.; Becker, H. C.; Wan, C.; Barton, J. K.; Zewail, A. H. *Angew. Chem., Int. Ed.* **2003**, *42*, 5896–5900.
- (13) Kelley, S. O.; Barton, J. K. *Science* **1999**, *283*, 375–381.
- (14) (a) Williams, T. T.; Dohno, C.; Stemp, E. D. A.; Barton, J. K. *J. Am. Chem. Soc.* **2004**, *126*, 8148–8158. (b) Valis, L.; Wang, Q.; Raychev, M.; Buchvarov, I.; Wagenknecht, H.-A.; Fiebig, T. *Proc. Nat. Acad. Sci. U.S.A.* **2006**, *103*, 10192–10195.
- (15) (a) Wagenknecht, H.-A.; Stemp, E. D. A.; Barton, J. K. *J. Am. Chem. Soc.* **2000**, *122*, 1–7. (b) Wagenknecht, H.-A.; Rajski, S. R.; Pascaly, M.; Stemp, E. D. A.; Barton, J. K. *J. Am. Chem. Soc.* **2001**, *123*, 4400–4407. (c) Dohno, C.; Stemp, E. D. A.; Barton, J. K. *J. Am. Chem. Soc.* **2003**, *125*, 9586–9587.
- (16) Stemp, E. D. A.; Arkin, M.; Barton, J. K. *J. Am. Chem. Soc.* **1997**, *119*, 2921–2925.
- (17) Nakatani, K.; Dohno, C.; Saito, I. *J. Am. Chem. Soc.* **2001**, *123*, 9681–9682.

N_4 -cyclopropylcytosine (^{CP}C)¹⁸ allows for probing transient hole and electron occupancy on DNA on a picosecond time scale. Model studies have shown that the cyclopropyl ring can open with a rate of $\sim 10^{11} \text{ s}^{-1}$ upon both oxidation and reduction.¹⁹ Thus these kinetically fast traps can report sensitively on transient occupancy of the DNA bridge for both HT and ET studies.

Our understanding today of DNA-mediated ET is far more rudimentary than DNA-mediated HT.²⁰ Early pulse radiolysis studies using noncovalently bound probes suggested a superexchange mechanism for electron transport at 77 K but perhaps thermally induced hopping at high temperature.²¹ Time-resolved transient absorption spectroscopic measurements indicated significantly better electron transfer to T than C in hairpin duplexes with the acceptor 2 bases from the donor.²² Covalently attached flavin analogues have been used by Carell and co-workers as photoreductants in assemblies where a thymine dimer was employed as the electron trap.²³ These studies showed little difference in repair efficiencies with T or C as the intervening bases in ET over 17 Å. Aromatic amines or pyrene-substituted uracil have also been employed as electron donors in DNA assemblies where 5-bromouracil (^{Br}U) was utilized as a fast kinetic electron trap.^{24–26} These studies did show variations depending upon sequence but only with a small distance (1–2 base pairs) for electron transport. It was observed that ET through intervening AT pairs is significantly more efficient than through GC segments; these results are reconciled by proton transfer between GC base pairs becoming rate limiting with fast traps as the reporter.

Our laboratory has examined DNA-mediated ET using DNA-modified electrodes.²⁷ Here, however, the DNA is linked to the electrode through a long alkane thiol linker, and it is transport through this linker that is rate-limiting.²⁸ Hence DNA electrochemistry experiments cannot be utilized to examine variations in DNA ET rates as a function of sequence or length. It is the case, however, that in these films, DNA ET can proceed over long molecular distances and in essentially a sequence-

independent manner.²⁷ In these studies, nonetheless, it is also apparent that DNA ET is very sensitive to coupling of the redox probe.²⁹

No studies have thus far utilized a single redox probe coupled effectively into the base pair stack to compare directly ET and HT in DNA. A uniform photoredox probe of appropriate binding and redox characteristics for both HT and ET must be developed for these experiments. Recently, several novel cyclometalated dipyrrophenazine (dppz) complexes of Ir(III) have been designed to trigger DNA redox reactions.³⁰ Here, we discuss studies using a cyclometalated Ir(III) complex, $[\text{Ir}(\text{ppy})_2\text{dppz}]^+$ (ppy = 2-phenylpyridine; dppz' = dipyrido[3,2-a:2',3'-c]phenazine-11-yl)-hex-5-ynoic acid), covalently tethered to DNA oligonucleotides. It has been shown that this complex has an excited-state oxidation potential of -0.9 V versus NHE and an excited-state reduction potential of 1.7 V versus NHE, which are sufficient to reduce pyrimidine and oxidize purine.^{30,31} ^{CP}C - and ^{CP}G -containing DNA are used to explore the resulting electron propagation process. This iridium intercalator serves as both an oxidant for HT and a reductant for ET upon photoactivation.

Experimental

DNA Oligonucleotides. All DNA oligonucleotides were synthesized using standard phosphoramidite chemistry on an ABI DNA synthesizer. N_2 -cyclopropyl-guanine (^{CP}G) and N_4 -cyclopropylcytosine (^{CP}C) modified sequences with the trityl group on were first prepared by solid-phase DNA synthesis, using 2-fluorinosine (^FI) and 4-thiouridine ($^{\text{Th}}\text{U}$) as precursors for the two substituted bases, respectively. The DNA oligonucleotides containing ^FI and $^{\text{Th}}\text{U}$ at the desired positions are then incubated in 6 M aqueous cyclopropylamine at 60 °C for 16 h for substitution reactions.³² ^{CP}C - and ^{CP}G -containing oligonucleotides are also cleaved from the resin during this incubation. The cleaved strands were purified by reverse-phase (RP) HPLC and repurified after removing the trityl group by treatment in 80% acetic acid for 15 min. Oligonucleotides were characterized by MALDI-TOF mass spectrometry.

The photoredox probe, $[\text{Ir}(\text{ppy})_2(\text{dppz}')^+]$ (ppy = 2-phenylpyridine; dppz' = (dipyrido[3,2-a:2',3'-c]phenazine-11-yl)-hex-5-ynoic acid), was synthesized using an ester derivative of $[\text{Ir}(\text{ppy})_2(\text{dppz}')^+]$ as the precursor, which was described previously.³⁰ The deprotection of the carboxylic acid was conducted in basic conditions. Briefly, the suspension of the ester-derived Ir(III) complex (0.5 mmol) in aqueous 0.4 M LiOH (50 mL) and THF (75 mL) was stirred at room temperature for 3 h. TLC (alumina 7% methanol/ CH_2Cl_2) was applied to monitor the reaction complete. The resulting mixture was adjusted to pH < 7 by 1.0 M HCl. The solvent was removed under reduced pressure, and the precipitates were collected by filtration and washed with copious water. The resulting solid was dissolved in 9 mL of 1:1:1 MeOH/ CH_2Cl_2 /MeCN and precipitated by 100 mL of ethyl ether and collected by filtration. Reversed-phase HPLC was applied to purify the crude product for characterization and spectroscopy. Crude product can be used for DNA coupling without further purification. The Ir(III) complex was characterized by ^1H NMR and mass spectrometry. Yield: 75%. ^1H NMR: (300 MHz, CD_2Cl_2): δ 9.85 (t, 2H, $J = 8.4 \text{ Hz}$), 8.50 (s, 1H), 8.42–8.34 (m, 3H), 8.05–7.94 (m, 5H), 7.82–7.41 (m, 4H), 7.48 (d, 2H, $J = 4.5 \text{ Hz}$), 7.14 (t, 2H, $J = 7.5 \text{ Hz}$), 7.05–7.02 (m, 2H), 6.42 (t,

- (18) Shao, F.; O'Neill, M. A.; Barton, J. K. *Proc. Natl. Acad. Sci. U.S.A.* **2004**, *101*, 17914–17919.
 (19) Musa, O. M.; Horner, J. H.; Shahin, H.; Newcomb, M. *J. Am. Chem. Soc.* **1996**, *118*, 3862–3868.
 (20) (a) Carell, T.; Meltzer, M. V. *Charge Transfer in DNA: From Mechanism to Application*; Wagenknecht, H. A., Ed.; Wiley: New York, **2005**, 77–91. (b) Wagenknecht, H.-A. *Angew. Chem., Int. Ed.* **2003**, *42*, 2454–2460.
 (21) (a) Cai, Z.; Li, X.; Sevilla, M. D. *J. Phys. Chem. B* **2002**, *106*, 2755–2762. (b) Li, X.; Cai, Z.; Sevilla, M. D. *J. Phys. Chem. B* **2001**, *105*, 10115–10123.
 (22) Lewis, F. D.; Liu, X.; Miller, S. e.; Hayes, R. T.; Wasielewski, M. R. *J. Am. Chem. Soc.* **2002**, *124*, 11280–11281.
 (23) (a) Schwögler, A.; Burgdorf, L. T.; Carell, T. *Angew. Chem., Int. Ed.* **2000**, *39*, 3918–3920. (b) Giese, B.; Carl, B.; Carell, T.; Behrens, C.; Hennecke, U.; Schiemann, O.; Feresin, E. *Angew. Chem., Int. Ed.* **2004**, *43*, 1848–1851. (c) Breeger, S.; Hennecke, U.; Carell, T. *J. Am. Chem. Soc.* **2004**, *126*, 1302–1303. (d) Manetto, A.; Breeger, S.; Chatgililoglu, C.; Carell, T. *Angew. Chem., Int. Ed.* **2006**, *45*, 318–321.
 (24) (a) Wagenknecht, H. A.; Fiebig, T. *Charge Transfer in DNA: From Mechanism to Application*; Wagenknecht, H. A., Ed.; Wiley: New York, **2005**, 197–223. (b) Kaden, P.; Mayer-Enthart, E.; Trifonov, A.; Fiebig, T.; Wagenknecht, H.-A. *Angew. Chem., Int. Ed.* **2005**, *44*, 1636–1639. (c) Wagner, C.; Wagenknecht, H.-A. *Chem. Eur. J.* **2005**, *11*, 1871–1876.
 (25) Rokita, S. E.; Ito, T. *Charge Transfer in DNA: From Mechanism to Application*; Wagenknecht, H. A., Ed.; Wiley: New York, **2005**, 133–151.
 (26) (a) Ito, T.; Rokita, S. E. *J. Am. Chem. Soc.* **2003**, *125*, 11480–11481. (b) Ito, T.; Rokita, S. E. *Angew. Chem., Int. Ed.* **2004**, *43*, 1839–1842.
 (27) (a) Kelley, S. O.; Jackson, N. M.; Hill, M. G.; Barton, J. K. *Angew. Chem., Int. Ed.* **1999**, *38*, 941–945. (b) Boon, E. M.; Drummond, T. G.; Hill, M. G.; Barton, J. K. *Nat. Biotechnol.* **2000**, *18*, 1096–1100.
 (28) Drummond, T. G.; Hill, M. G.; Barton, J. K. *J. Am. Chem. Soc.* **2004**, *126*, 15010–15011.

- (29) Gorodetsky, A. A.; Green, O.; Yavin, E.; Barton, J. K. *Bioconjugate Chem.* **2007**, *18*, 1434–1441.
 (30) Shao, F.; Elias, B.; Lu, Wei.; Barton, J. K. *Inorg. Chem.* **2007**, in press.
 (31) (a) Steenken, S.; Jovanovic, S. V. *J. Am. Chem. Soc.* **1997**, *119*, 617–618. (b) Steenken, S.; Telo, J. P.; Novais, H. M.; Candeias, L. P. *J. Am. Chem. Soc.* **1992**, *114*, 4701–4709.
 (32) Shao, F.; Augustyn, K. E.; Barton, J. K. *J. Am. Chem. Soc.* **2005**, *127*, 17445–17452.

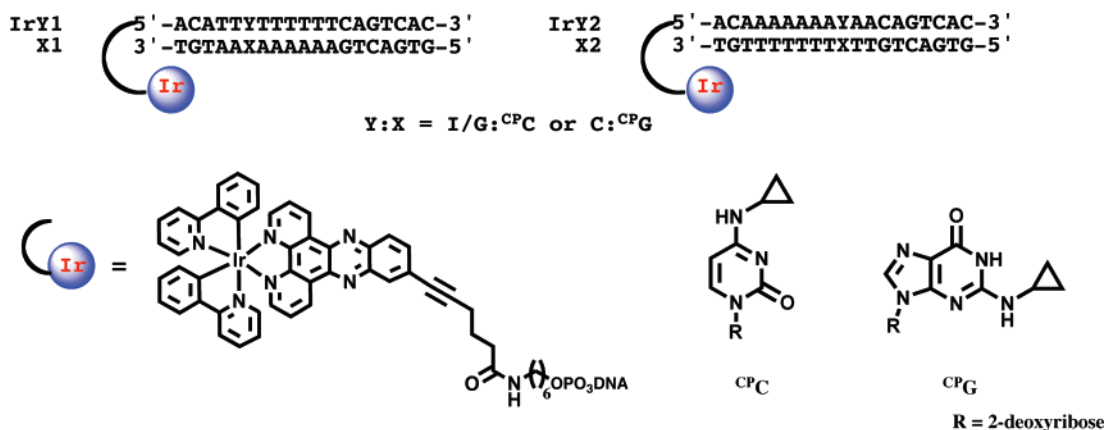


Figure 1. Ir(III)-tethered DNA assemblies used in the DNA-mediated photoredox reactions. The Ir complex serves as both photooxidant and photoreductant and is tethered to the DNA oligonucleotide by a C₆-alkyl amino-linker through a phosphate linkage. Cyclopropylamine-substituted nucleosides, ^{CPc} and ^{CPg}, are incorporated in the complement of the Ir-tethered strands as fast kinetic electron and hole traps, respectively. Structures of the cyclometalated Ir(III) complex and cyclopropylamine-modified bases are shown below.

2H, $J = 7.8$ Hz), 2.66~2.61 (m, 4H), 2.04~1.97 (m, 2H). ESI-MS: calcd, 893.2216 for C₄₆H₃₂N₆O₂Ir; found, 893.2198.

[Ir(ppy)₂(dppz')]⁺ was covalently tethered to DNA oligonucleotides as follows. First, the detritylated resin-bound oligonucleotides with an amine-ended C₆-alkyl linker were prepared by phosphoramidite chemistry. The amine-modified strands were then reacted with [Ir(ppy)₂(dppz')]⁺ in anhydrous DMF using *O*-(benzotriazol-1-yl)-*N,N,N',N'*-tetramethyluronium hexafluorophosphate (HBTU, Aldrich) and 1-hydroxybenzotriazole hydrate (HOBT, Aldrich) as the coupling reagent in the presence of diisopropylethylamine (DIEA). Cleavage from the resin was accomplished by incubation in NH₄OH at 60 °C for 6 h. Strands were HPLC-purified using a Varian C₄ reversed-phase column. MALDI-TOF mass spectrometry was used to characterize the metalated DNA conjugates. For example, calcd, 6557 for **IrG2** (C₅₂H₄₄N₇O₅PIr-5'-ACAAAAAGAACAGTCAC-3'); found, 6556 for (M-H)⁻. DNA oligonucleotides were suspended in buffered aqueous solution (10 mM sodium phosphate, 20 mM NaCl, pH 7) and quantitated by UV-visible spectroscopy.

Melting Temperatures. Melting temperatures (T_m) of all the duplexes were measured using a Beckman DU 7400 spectrophotometer with a temperature control attachment. Absorption at 260 nm (A_{260}) of equimolar DNA complements (1.5 μM in 10 mM NaCl, 20 mM sodium phosphate, pH 7.0) were measured every 0.5 °C from 90 to 15 °C with rate 0.5 °C/min. The reverse temperature traces were measured under the same conditions to confirm the reversibility of the DNA annealing process. The data were fit to a sigmoidal curve to determine the T_m . The absorption profile was also measured at 413 nm (A_{413}) as a function of temperature for 20 μM Ir(III)-tethered DNA aliquots in the same buffer in order to measure the corresponding T_m of the Ir(III) complex within the duplex. The error of T_m over at least three sets of individual experiments was less than 1 °C.

Photolysis Experiments. Aliquots (10 μM DNA, 30 μL) for irradiation were prepared by annealing equimolar amounts of the desired DNA complements on a DNA thermal cycler (Perkin-Elmer Cetus) from 90 to 15 °C over a period of 2.5 h. Aliquots of the Ir-tethered duplexes were then irradiated with a 1000W Hg/Xe lamp equipped with a 320 nm LP filter and a monochromator. After irradiation at 380 nm (0, 30 min, 60 min), duplex samples were digested by 37 °C incubation with phosphodiesterase I (USB) and alkaline phosphatase (Roche) for 24 h to yield the free nucleosides, and the samples were analyzed by reversed phase HPLC (Chemcobond 5-ODS-H, 4.6 × 100 mm). The percentage decomposition (Y) of cyclopropyl-modified bases was determined by subtracting the ratio of the area under the ^{CPg} or ^{CPc} peak in an irradiated sample from that in a nonirradiated sample, using adenine as an internal standard for all HPLC traces. Irradiations were repeated three times, and the results were averaged.

Table 1. Sequence and Melting Temperatures of DNA Assemblies in the Studies of DNA-Mediated ET and CT upon Irradiation of the Tethered Ir(III) Complex

DNA	sequence	T_m (DNA) (°C) ^a	T_m (Ir) (°C) ^b
IrG1 ^c ^{CPc} 1	Ir-5'-ACATT-GTTTTTTCAGTCAC-3' 3'-TGTAAC ^{CPc} CAAAAAAGTCAGTG-5'	53	61
set no. 1	IrI1 ^{CPc} 1	50	60
IrC1 ^{CPg} 1	Ir-5'-ACATT-CTTTTTTCAGTCAC-3' 3'-TGTAAC ^{CPg} GAAAAAGTCAGTG-5'	53	59
IrG2 ^{CPc} 2	Ir-5'-ACAAAAA-GAACAGTCAC-3' 3'-TITTTTTT ^{CPc} CTTGTCAAGTG-5'	49	55
set no. 2	IrI2 ^{CPc} 2	47	52
IrC2 ^{CPg} 2	Ir-5'-ACAAAAA-CAACAGTCAC-3' 3'-TITTTTTT ^{CPg} GTTGTCAAGTG-5'	51	57
G1 ^{CPc} 1	5'-ACATT-GTTTTTTCAGTCAC-3' 3'-TGTAAC ^{CPc} CAAAAAAGTCAGTG-5'	47	

^a T_m is determined by monitoring the UV absorption of 1.5 μM DNA in 20 mM sodium phosphate, pH 7.0, 10 mM NaCl at 260 nm from 90 to 15 °C. ^b T_m is determined by monitoring UV absorption of 20 μM DNA in 20 mM sodium phosphate pH 7.0, 10 mM NaCl at 413 nm from 90 to 15 °C. ^c Ir represents the covalently tethered complex [Ir(ppy)₂dppz']⁺.

Results and Discussion

Experimental Design. The modified DNA assemblies utilized for these studies are shown in Figure 1. Upon photolysis, the tethered cyclometalated Ir(III) complex serves as both a photooxidant and a photoreductant for ET and CT in the assemblies. Cyclopropylamine-modified bases, ^{CPc} and ^{CPg}, are employed as fast kinetic traps to probe the transient electron and hole densities during both electron migration processes. The Ir(III) complex is covalently tethered to the complementary strand of the cyclopropyl-substituted DNA oligonucleotide through a C₆-alkyl linker. Here, the alkyl chain is connected to the 5'-end of DNA single strands through a phosphate linkage, which may better mimic the DNA backbone than the diamine alkyl linker used in Rh(III)-tethered DNA.^{4,18}

Two sets of DNA duplexes were prepared here to explore long-range redox chemistry between the tethered Ir(III) complex and DNA (Table 1). All the duplexes have a three base pair

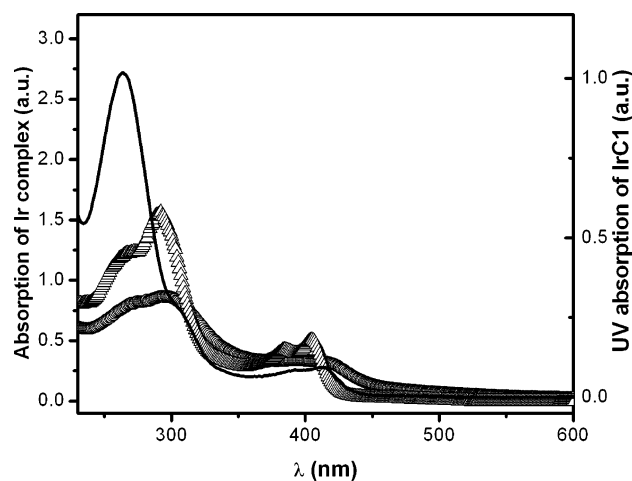


Figure 2. UV–visible spectra of Ir–DNA conjugates and the free $[\text{Ir}(\text{ppy})_2\text{dppz}]^+$ complex. Free Ir(III) complex ($23 \mu\text{M}$) in MeCN (triangle) and buffer (circle) (10 mM NaCl, 20 mM sodium phosphate, pH 7.0), as well as tethered to the DNA single strand **IrC1** (black line, $4.5 \mu\text{M}$) in buffer, are used to measure the spectra.

segment, 5′-ACA-3′ at the metal-tethering end to accommodate the intercalative dppz′ ligand. An eight-base pair (bp) adenine tract follows the intercalation site to study the potential DNA-mediated ET and HT through the A-tract. On the distal side of the A-tract, a mixed seven-base sequence is included and is constant to minimize any effects of fraying ends in the duplexes. In set no. 1, 8 adenines are placed in strands that are complementary to the Ir(III) tethered strands (**IrY1**, $Y = \text{I, G, or C}$). Cyclopropyl-substituted bases, ^{CP}C and ^{CP}G are placed after the second adenine in ^{CP}C1 and ^{CP}G1, respectively. DNA assemblies in set no. 2 (**IrY2**, $Y = \text{I, G, or C}$) have the same A-tract, but the purine and pyrimidine strands are flipped between the complements. ^{CP}C and ^{CP}G are placed after the fifth thymine in the A-tract in the corresponding sequences of set no. 2. Inosines are also included to enhance the efficiencies. These two sets of Ir-tethered DNA assemblies would allow us to compare the transient hole and electron distributions between the purine and pyrimidine strands during DNA-mediated HT and ET, respectively.

Intercalation of the Tethered Ir(III) Complex. UV–visible spectra of the Ir(III)-tethered DNA (Ir–DNA) have characteristic bands at 260 nm, primarily from the DNA bases, and around 380–430 nm from a mix of intraligand transitions of dppz and the metal-to-ligand charge transfer (MLCT) band of the Ir complex.³³ As is evident in Figure 2, the absorption spectrum of $[\text{Ir}(\text{ppy})_2\text{dppz}]^+$ shows significant solvatochromic effects. Hypochromicity and broadening are observed at both the high energy intraligand and the low-energy bands in changing from organic solvent to aqueous buffered solution. Upon tethering to the DNA single strand, the features of the absorption spectrum of the Ir(III) complex in the low-energy band can be resolved in aqueous buffer, however. The maximum absorption for the low-energy band in Ir–DNA appears in between those of Ir(III) in buffer and acetonitrile. Two absorption maxima at 393 and 413 nm, which are broadened out in aqueous solution, are present to some extent in the case of Ir–DNA, although they are still not well resolved and have been red-shifted ~ 10 nm compared to MeCN. The spectral features of the Ir complex

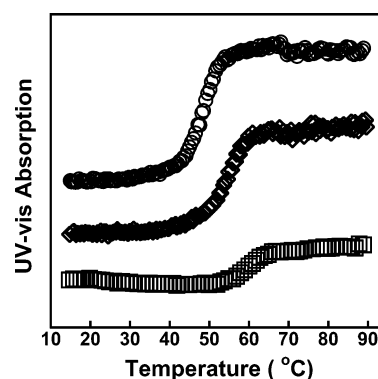


Figure 3. Melting temperatures of DNA duplexes with or without the tethered Ir(III) complex: (top) $1.5 \mu\text{M}$ G-1/^{CP}C-1; (middle) $1.5 \mu\text{M}$ IrG-1/^{CP}C-1; (bottom) $20 \mu\text{M}$ IrG-1/^{CP}C-1. The UV absorption is monitored at 260 nm for $1.5 \mu\text{M}$ DNA assemblies and at 413 nm for $20 \mu\text{M}$ IrG-1/^{CP}C-1. Shown are both annealing and remelting curves, which are superimposable.

upon tethering to DNA, in particular the hypochromicity, suggests that the dppz′ may stack, at least partially, with the nucleic acid bases even in the single DNA strands, which, to some extent, may create an environment more like acetonitrile than water.

Melting temperatures of Ir–DNA assemblies also provide evidence of intercalative stacking to stabilize the tethered duplex. Melting temperatures ($T_m(\text{DNA})$) of DNA assemblies ($1.5 \mu\text{M}$) in set no. 1 are found at $50 \sim 52 \text{ }^\circ\text{C}$, as well as set no. 2 at $47 \sim 51 \text{ }^\circ\text{C}$, by monitoring the characteristic A_{260} associated with base stacking from $90 \text{ }^\circ\text{C}$ to $15 \text{ }^\circ\text{C}$ reversibly. The samples were heated at $90 \text{ }^\circ\text{C}$ for 5 min, then cooled slowly by $0.5 \text{ }^\circ\text{C}/\text{min}$ and the spectra were monitored. Remelting ($0.5 \text{ }^\circ\text{C}/\text{min}$) shows the melting curves to be superimposable. As shown in Figure 3 and Table 1, **IrG1/CP-C1** has a T_m that is $5 \text{ }^\circ\text{C}$ higher than the same DNA sequence without tethered Ir(III), **G1/CP-C1**. Furthermore, the absorption intensities at the MLCT band of Ir(III)-DNA were measured at 413 nm following the same temperature cycle. By fitting the data to a sigmoidal curve, the $T_m(\text{Ir})$ (temperature at half-maximum of A_{413}) can be obtained to characterize the melting of the Ir(III) complex from the DNA duplex. The $T_m(\text{Ir})$'s of Ir–DNAs are observed around $60 \text{ }^\circ\text{C}$ for set no. 1 and $55 \text{ }^\circ\text{C}$ for set no. 2 as shown in Table 1. Remarkably, the $T_m(\text{Ir})$ increases an extra $7 \sim 8 \text{ }^\circ\text{C}$ from the $T_m(\text{DNA})$ of the same assemblies.³⁴ Interestingly, in the DNA assembly with a $[\text{Ru}(\text{phen})_2\text{dppz}]^{2+}$ complex covalently tethered to DNA through a carboxylic acid functional group on the intercalative dppz ligand, similar T_m enhancement was observed and assigned to stabilization of the duplex because of the intercalation of dppz.³⁵ Thus, the increase in $T_m(\text{Ir})$ indicates that the Ir complex stabilizes the end of the DNA duplex from separating even after much of the duplex has been denatured. Certainly the duplex stabilization and the hypochromicity in the MLCT band support the idea that the tethered Ir(III) complex can adopt an intercalation mode. The reversibility of the melting curves suggests that threading to achieve intercalation is feasible.

(34) Although $20 \mu\text{M}$ solution of DNA samples, instead of $1.5 \mu\text{M}$, are used in the $T_m(\text{Ir})$ experiment to achieve measurable absorption intensities, the enhancement due to the concentration increments should be less than $4 \text{ }^\circ\text{C}$.

(35) (a) Kitamura, Y.; Ihara, T.; Okada, K.; Tsujimura, Y.; Shirasada, Y.; Tazaki, M.; Jyo, A. *Chem. Commun.* **2005**, 4523–4525. (b) Ossipov, D.; Pradeepkumar, P. I.; Holmer, M.; Chattopadhyaya, J. *J. Am. Chem. Soc.* **2001**, *123*, 3551–3562.

(33) Lo, K. K.; Chung, C.; Zhu, N. *Chem. Eur. J.* **2006**, *12*, 1500–1512.

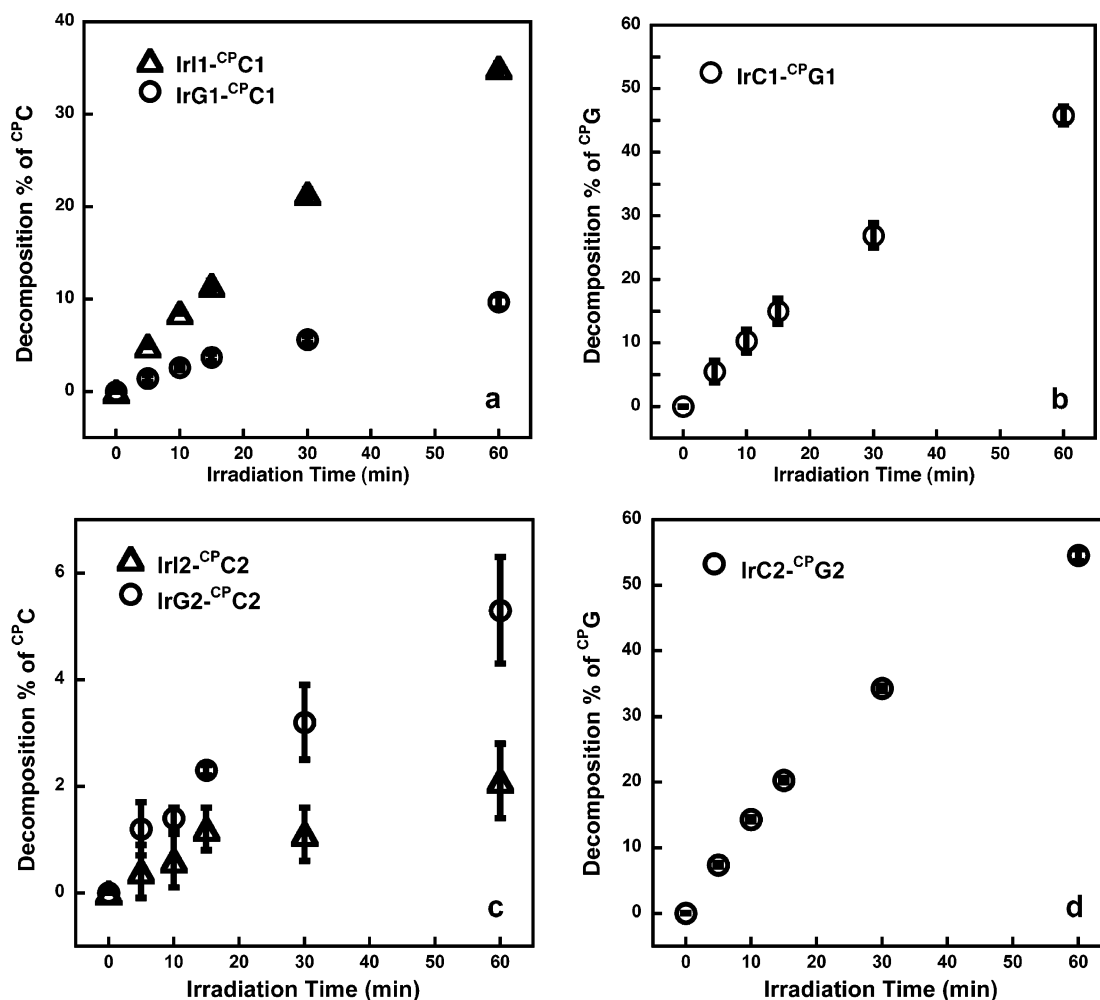


Figure 4. Redox decomposition of cyclopropylamine-substituted DNA assemblies upon irradiation of the tethered Ir(III) complex. Percentages of decomposition of ^{Cp}C in assemblies set of no. 1 (top left) and no. 2 (bottom left), as well as those of ^{Cp}G in set no. 1 (top right) and no. 2 (bottom right). The error bars are obtained over 3 sets of individual experiments.

DNA-Mediated Hole Transport by Photoexcited Ir(III). DNA assemblies in set no. 1 have either a ^{Cp}C or a ^{Cp}G positioned within the A-tract five base pairs away from the Ir-tethering end. Upon irradiation of Ir(III) at 380 nm, in these assemblies both cyclopropylamine-substituted bases are seen to decompose linearly with an irradiation time of ≤ 1 h as shown in Figure 4. In IrC1-^{Cp}G1, 46% of ^{Cp}G is decomposed after 1 h by the irreversible oxidative ring-opening reaction. ^{Cp}C decomposition is also observed in both assemblies, IrI1-^{Cp}C1 and IrG1-^{Cp}C1. Notably, however, duplex IrI1-^{Cp}C1 exhibits more efficient decomposition (35% after 1 h) than does IrG1-^{Cp}C1 (10% after 1 h). The enhanced ^{Cp}C decomposition in the duplex with base pairing to inosine, a guanine derivative of higher oxidation potential, is a characteristic feature of ^{Cp}C oxidation.¹⁸ The higher ring-opening yield observed in IrI1-^{Cp}C1 versus IrG1-^{Cp}C1 is explained by the less competition from the paired base for the hole occupancy on ^{Cp}C within the inosine-containing assembly versus the guanine-containing assembly. Efficient photooxidation of ^{Cp}C by the Ir complex might be somewhat surprising based upon the excited-state reduction potential of the Ir complex ($E_{\text{red}}^* = 1.7$ V vs NHE); the driving force would be very small, at best.³⁰ However, previous studies have shown that purine stacking in the duplex can significantly lower the oxidation potentials of the DNA

bases.^{36,37} Thus it is reasonable to consider that the oxidation potential of ^{Cp}C in IrI1-^{Cp}C1 and IrG1-^{Cp}C1 is lowered enough to be oxidized by the excited-state of the Ir complex. With photoactivation, then, using this tethered photooxidant both ^{Cp}G and ^{Cp}C can be oxidized from a distance through DNA-mediated HT.

DNA-Mediated Electron Transport by Photoexcited Ir(III). In set no. 2 versus set no. 1, with respect to the Ir(III)-tethered end, the A-tract is flipped between the two complementary strands. ^{Cp}G and ^{Cp}C are thus positioned in the pyrimidine strands of the A-tract and are located after the sixth thymine (Table 1). In this set of assemblies, oxidative decomposition of ^{Cp}G in IrC2-^{Cp}G2 is observed upon irradiation at 380 nm and has comparable efficiency (55% after 1 h) to that of IrC1-^{Cp}G1. Photoexcitation of the Ir complex in set no. 2 thus shows similar decomposition yields to set no. 1. As expected, the electronic coupling between the bound Ir complex and the DNA base pairs certainly is not changed and the variation in yield with distance is shallow.

Significantly, ^{Cp}C in both IrI2-^{Cp}C2 and IrG2-^{Cp}C2 are also decomposed upon irradiation of a distally tethered Ir(III)

(36) Voityuk, A. A.; Jortner, J.; Bixon, M.; Rösch, N. *Chem. Phys. Lett.* **2000**, *324*, 430–434.

(37) Sugiyama, H.; Saito, I. *J. Am. Chem. Soc.* **1996**, *118*, 7063–7068.

complex, but now the efficiency of charge transport in the inosine-containing duplex is equivalent to or lower than that of the guanine-containing duplex (Figure 4). Decomposition efficiencies of ${}^{\text{CP}}\text{C}$ in this series are significantly lower than for series no. 1 where the ${}^{\text{CP}}\text{C}$ is embedded within the purine strand. The increased separation from the Ir center might be considered a contributor to the lowered efficiency, but the switch in efficiency between the guanine-containing duplex and the inosine-containing duplex indicates that a different mechanism for charge transport must be involved. A similar phenomenon is observed in the case of photoactivation of a platinum diimine complex with ${}^{\text{CP}}\text{C}$ -containing duplexes.³⁸ The switch to give greater decomposition with ${}^{\text{CP}}\text{C}$ paired to guanine versus inosine supports the idea that for the transport through pyrimidines it is ET that is preferred. In the pyrimidine series, no. 2, ${}^{\text{CP}}\text{C}$ is reduced by the excited-state of the distally bound Ir. The flanking pyrimidines likely do not efficiently decrease the oxidation potential of ${}^{\text{CP}}\text{C}$ by base stacking,³⁶ and the pyrimidine bridge provides a viable low-energy path for electron transport. Hence, in the ${}^{\text{CP}}\text{C}$ -containing duplexes of set no. 2, the reductive ring opening reaction of ${}^{\text{CP}}\text{C}$ effectively competes with ${}^{\text{CP}}\text{C}$ oxidation. Therefore, upon direct irradiation, the covalently tethered Ir(III) can promote both DNA-mediated HT and ET, probed by decomposition of ${}^{\text{CP}}\text{G}$ and ${}^{\text{CP}}\text{C}$.

These results must be considered in the context also of other studies of DNA charge transport. Purine strands are known to be more effective conduits for HT than pyrimidine strands, although the full sequence of the duplex, before and after the trap, contributes to the transport efficiencies.³² For ET, extensive studies have not been carried out as a function of distance and

sequence. Indeed, only differences in transport efficiencies between T and C as the intervening bridge have been explored.^{23–26} For ET, effective traps and well-coupled electron donors are needed to achieve ET over sufficient distances where, as for HT, sequence variations could become significant. Certainly, the relative reduction potentials for pyrimidines versus purines make our observations of a preference for electron transport within a pyrimidine bridge and hole transport within a purine bridge understandable.

Summary and Implications. A cyclometalated Ir(III) complex has therefore been covalently tethered to DNA oligonucleotides and provides both a photooxidant and photoreductant for studying DNA-mediated HT and ET. Melting temperatures monitored at both the DNA absorption band and the MLCT band of Ir(III) indicate stabilization of the DNA duplex by the tethered complex, consistent with intercalation by the functionalized dppz. Thus the Ir complex can provide consistent and effective electronic coupling with the DNA base pairs for both HT and ET. Upon photolysis, both the reduction of ${}^{\text{CP}}\text{C}$ and oxidation of ${}^{\text{CP}}\text{G}$ are promoted by DNA-mediated ET and HT from the distally DNA-bound Ir(III). Therefore, ET and HT can be initiated with the same photoredox probe and can be probed on a picosecond scale by ring-opening of cyclopropyl amine-substituted bases. The Ir–DNA assembly is a unique model system that allows us now to compare characteristics of DNA-mediated HT and ET directly in the same donor–bridge–acceptor system.

Acknowledgment. We are grateful to the NIH (Grant GM49216) for their financial support of this work.

(38) Lu, W.; Vicic, D. A.; Barton, J. K. *Inorg. Chem.* **2005**, *44*, 7970–7980.

JA0752437